Acta Cell Biologica Open Access

Spring (2025) 1(1): 17-31

ORIGINAL ARTICLE

Identification of a novel Cyc2 mutation (F312Y) to predict the stability of protein structure by molecular dynamic

Somayeh Farahmand[1], Marzieh Dehghan Shasaltaneh[2(ORCID: 0000000214257347)], Faezeh Fatemi[3], Mahnaz Shojapour[1]

1. Department of Biology, Payame Noor University (PNU), Tehran, Iran.
2. Department of Biology, Faculty of Science, University of Zanjan, Zanjan, Iran.
3. Materials and Nuclear Fuel Cycle Research School, NSTRI, Tehran, Iran.

Correspondence:
Marzieh Dehghan Shasaltaneh
Email: dehghan@znu.ac.ir

Received: 7/May/2023
Accepted: 12/Nov/2023

How to cite:
Farahmand, S., Dehghan Shasaltaneh, M., Fatemi, F., & Shojapour, M. (2025). Identification of a novel Cyc2 mutation (F312Y) to predict the stability of protein structure by molecular dynamic. *Acta Cell Biologica*, 1 (1), 17-31.

ABSTRACT

Iron-rusticyanin reductase (Cyc2) is the first protein in the respiratory chain of *Acidithiobacillus ferrooxidans (Af)*, which plays a crucial role in electron transfer. Cytochrome c (cytC) is located in the bacterial outer membrane (OM) and functions as the first electron carrier inside the respiratory ferrous iron oxidation pathway is encoded by the *Cyc2* gene. The present computational research examines the effect of a novel Cyc2 mutation (F312Y) to enhance conformational flexibility of the mentioned protein for target recognition. Molecular dynamic simulations (MD) of wild and mutant types of Cyc2 protein were carried out. By analyzing RMSD, RMSF, SASA, Rg, H Bond, DSSP, PCA, ED, DCCM, FEL and EM the conformational variations of mutated protein were studied. The results of the RMSF analysis represent an increase in the flexibility of the ligand after mutant. Eventually, the flexibility of the active site probably improves electron transfer by increasing the amount of E_o at the mutation point. Our results confirm that the mutated protein retains its stability during the simulation. With the conversion of Phenylalanine 312 into Tyrosine, an alpha-amino acid with hydrophobic and nonpolar side chains changes to a polar side group with an extra -OH group. This resulted in more intracellular hydrogen bonds. Furthermore, the mutant variant was more stable than the wild-type. Findings from the present study indicate that an interface between the F312Y mutation and rusticyanin activation could improve the electron transfer rate and yield fruitful insight into site-specific mutagenesis studies.

KEYWORDS

Acidithiobacillus ferrooxidans, Cytochrome c, Molecular Dynamics Simulation, Point Mutation; Respiratory Chain.

1. Introduction

Cyc2 is the first protein in the respiratory chain of the *Acidithiobacillus ferrooxidans* bacterium, playing an imperative role in electron transfer. These bacteria are involved in a bioleaching process in which metals are extracted from ores. If the ore does not have enough metal to be extracted through chemical methods, then bioleaching is a suitable technique. *Acidithiobacillus ferrooxidans*, is among the highly valuable bacteria that primarily use sulfur or iron oxidation (Fe2+) compounds as its energy source (Yarzábal *et al*., 2002). The Cyc2 protein, placed in the outer membrane, encodes the cytochrome c and hence it could be the first electron transporter inside the respiratory ferrous iron oxidation pathway (Valdés *et al*., 2008). Complex IV (COX), attached to the plasmalemma, acts as the electron acceptor. Electron transfer takes place via a group of periplasmic proteins, inclusive of copper proteins, RCy, and at least one cytC (Yarzábal *et al*., 2002). It has been determined that RCy, Cyc1, Cyc2, and aa_3-type cytC oxidase are essential components of the ferric iron oxidation system. Biochemical studies have shown that the high molecular weight Cyc2 in OM oxidizes Fe^{2+} followed by transportation of the electrons to O_2 through RCy, periplasmic Cyc1, and eventually Cox domain in the internal membrane (IM) (Quatrini *et al*., 2006). Finally, these proteins produce a water molecule via O_2 reduction (Lyons *et al*., 2012). Recently, it has been suggested that the proteins needed for downhill pathway transfer of electrons are ordered as supercomplexes that are located in the OM, IM, and periplasm (Patra *et al*., 2013). However, the character and subcellular localization of the primary electron acceptor from ferrous sources remain undetermined (Yarzábal *et al*., 2002, Er *et al*., 2011, Abriata 2018). Similar to many membrane proteins, studying Cyc2 in the laboratory is quite challenging, and as of now, there is no available structure that can be used as a template for modeling. The Cyc2 has four sections made up of a signal peptide, a cytochrome-like haem-binding domain, a flexible protein linker, and a large transmembrane beta-barrel domain. The beta-barrel and cytochrome-like haem-binding domains connect via a flexible protein linker. The cytochrome-like domain may be present in three possible places (in the periplasm or outer cell space, and within the β-barrel domain) (Abriata, 2018) to oxidize Fe^{2+} and obtain electrons from it, then give it to proteins such as RCy in the periplasm. The secondary structure likely includes an N-terminal alpha-helix that aligns with the presumed targeting signal, followed by three shorter helices and multiple β-strands (Abriata, 2018). Due to various interactions between haem and the surrounding amino acids, haem-containing proteins carry out many biological functions. In *A. ferrooxidans*, the haem C group of Cyc2 performs an important biological function in transporting the electrons released by Fe^{2+} oxidation. One of the residues, Phe312 of the outer membrane resided cytochrome C, performs an important part in the diffusion of the stream of electrons from haem C group to Asp73 of RCy (Patra *et al*., 2013). The hydrophobic residues on the external side of the barrel, along with the polar residues at its surface are introduced as an integral membrane protein (IMP). Cytochrome-like domain has three sizes of 25, 20, and 20 Å; hence it could fit inside the β-barrel domain or in the periplasm, either resting or with the liberty to skip through the region in the extracellular membrane localization. In the first case, the static ferrous oxide enters the barrel and delivers the electrons from its base to the periplasmic surface, so the downstream electron receptor protein should be placed there. In the second situation, the dynamic Cyt-like domain can float about in the barrel to catch ferrous

oxide ions from the outside, after which releases them across the barrel in the direction of the periplasm. In other words, the Cyt-like domain is in two feasible places: exposed to the periplasm or outer cell space, or docked inside the β-barrel domain. It is essential that the two electron receivers from Cyc2, RCy, and Cyc4 would not be placed in the Cyc2 barrel (Yarzábal *et al*., 2002; Valdés *et al*., 2008; Patra *et al*., 2013; Abriata, 2018).

Gooley *et al*. (1992) demonstrated that converting Tyr to Phe through mutation resulted in a decrease of 59 mV in the redox potential (Gooley *et al*. 1992). Similarly, Kolling *et al*. (1993) found that substituting Tyr with Phe156 led to a reduction of 45 mV in the redox potential (Kolling *et al*., 2007). Given the above two sentences, the mutation of Phe to Tyr can increase the redox potential. We selected this specific mutation due to the extra hydroxyl group in tyrosine compared to phenylalanine, which can enhance intramolecular hydrogen bonding. Also, The Hot Spot server suggested F312Y for mutation. Therefore, there is a greater tendency to receive electrons from heme C and, improve the electron transfer speed.

2. Materials and Methods

2. 1. Homological Based Modeling and its Validation

The sequence of Cyc2 protein containing 485 amino acids was obtained out of the Universal Protein Resource (UniProt, http://www.uniprot.org) (Id code: B7JAQ7). But it has no crystallographic structure. A template structure of Cyc2 protein (PDB ID: 2WJQ) with a resolution of 2.00 Å was used for homology modeling using Modeler software (version 9.1.2). The best pdb file was selected according to DOPE. To validate the structural integrity of both the wild-type and mutant forms, several servers were utilized, including ProSA-web (https://prosa.services.came.sbg.ac.at), QMEAN (http://swissmodel.expasy.org/qmean), Verify 3D (http://servicesn.mbi.ucla.edu/Verify3d/) along with RAMPAGE (http://mordred.bioc.cam.ac.uk/~rapper/rampage.php) (Ghasemi *et al*., 2016).

2. 2. In Silico Mutation Analysis

The web-version of DUET (http://biosig.unimelb.edu.au/duet/stability), iStable (http://predictor.nchu.edu.tw/iStable/), I-Mutant2.0 (http://folding.biofold.org/cgi-bin/i-mutant2.0.cgi) along with MUpro (http://mupro.proteomics.ics.uci.edu/) servers were used for the prediction of protein stability upon point mutations (single amino acid substitution).

DUET is a web server that predicts the changes in protein stability (ΔΔG) via an integrated computational approach (Pires *et al*., 2014). The server iStable is an integrated analyzer of protein stability modifications upon single mutations (Chen *et al*., 2013). MUpro functions as a server that predicts protein stability variations for single-site mutations from sequences (Cheng *et al*., 2006). I-Mutant2.0 acts as a tool for prediction of protein stability upon single point mutations from the protein sequence and structure (Capriotti *et al*., 2005).

2. 3. Simulation System Setup

Cytochrome c2 was inserted into a lipid bilayer consisting of 38592 POPC lipids followed by equilibration for 100 ns MD simulations using GROMACS (v 2021.2). The Simulation of POPC bilayer was performed applying Amber force field ff99SB. Proteins wild and mutant were each placed separately in a simple cubic box with dimensions of 17.38×17.38×17.38 nm (Pearlman *et al*., 1991). Additionally, through the deletion of POPC molecules, a

hole with an identical proportion as the protein location was created in the lipid bilayer (Faraldo-Gómez *et al*., 2002). Then, a computer simulation run was performed wherein the lipid molecules at the perimeter of the hole were faced with forces perpendicular to a molecular surface, brought about from the protein insertion. Then, Na^+ and Cl^- ions with SPC water molecules were added to neutralize all systems (Berendsen *et al*., 1981). After 5000 steps of energy minimization (Jafari and Mehrnejad 2016), MD simulation was run in NVT and NPT groups. Periodic border settings were engaged in all three directions (x, y, and z).

The SPC model represented water. Temperature was kept constant at 300 K while 1 bar pressure was fixed using the modified Berendsen algorithm (Berendsen *et al*., 1984). To confine bond lengths, the atomic positions and velocities were saved every 50,000 ps using the LINCS algorithm. A time step of 2 fs was used to determine the conformational changes of Cyc2 protein (Hess *et al*., 1997).

2. 4. Trajectory Analysis

Molecular dynamics simulation data were analyzed using the obtained trajectory files together with structural behavior. Moreover, a comparative analysis for the wild and mutant types was conducted. During the simulation root-mean-square deviation (RMSD), root-mean-square fluctuation (RMSF), radius of gyration (Rg), solvent-accessible surface area (SASA), hydrogen bonds (H-bond), distance and thickness, Define Secondary Structure of Proteins (DSSP) analysis, principal component analysis (PCA), essential dynamics (ED), dynamic cross correlation map (DCCM) and free energy landscape (FEL) were determined. Principal components analyses (PCA) of Cα atoms of all systems were performed to distinguish the crucial motions following the simulation of conformational transitions. The analyses were performed using the approach from Amadei *et al*., and de Groot *et al*., in which a covariance matrix of Cα atomic fluctuation (C) was constructed to give eigenvectors and the corresponding eigenvalues, where eigenvectors indicate the direction of motion along the principal components, and the corresponding eigenvalues denote the mean square fluctuations related to the principal components (Bekker *et al*., 1993, Berendsen *et al*., 1995, Lindahl *et al*., 2001, Van Der Spoel *et al*., 2005). Essential Dynamics (ED) is a common application of principal component analysis (PCA). Subsequent to the determination of dispersion matrix made from fluctuations of atomic positions in the trajectory, a set of eigenvectors and corresponding eigenvalues were generated. Essential dynamics is a powerful analysis to compare ED characteristics of two simulations on almost identical systems. In our research, we conducted combined ED on a trajectory made by concatenating the F312Y-mutant together with wild-type from the MD trajectories. Comparing and analyzing the properties of various sections of the projection throughout the length of the combined eigenvector impart a potential method to evaluate similarities and differences in equilibrium between these two systems (Amadei *et al*., 1993, Balsera *et al*., 1996). For the time correlation motion detection of all pairs of Cα atoms between the wild and F312Y-mutant systems, Dynamic cross correlation map (DCCM) analyses were employed (Ichiye and Karplus 1991). Free energy landscape (FEL) represents the possible distribution as an outcome of the varying element(s) of the protein system that assists one to envisage the permanence of different protein conformations. The permanence of the protein is explained in terms of Gibb's free energy. It is a function of the enthalpy-entropy compensation of protein that

analyzes the different conformational states, which plays a significant role in structure-function correlation of proteins. Determinations of free-energy values for backbone atoms of both wild and F312Y-mutant systems were executed using GROMACS (Amadei *et al*., 1993, De Groot *et al*., 1996).

2. 9. Statistical analysis

Our results were analyzed using SPSS v19.0 and presented as mean ± standard error of the mean (SEM). All facts and figures were assessed using a t-test, and statistically significant resluts were accepted at $p<0.05$.

3. Results

3. 1. Homology-Based Modeling of Wild-Type and Mutant Structures

The results of PorSA-web and QMEAN Z-score indicated that the models have the desirable qualities. Besides, Verify 3D had an averaged 3D-1D score≥ 0.2 and RAMPAGE showed residues in the allowed region (Ghasemi *et al*., 2016). Subsequently, protein stability was assessed using four servers including DUET, I-Mutant2, MUpro, and istable that are presented in Table 1. The results illustrated the stability of the protein structure after mutation. The three-dimensional protein structures of the wild-type and F312Y mutant were visualized using PyMOL (http://sourceforge.net/projects/pymol/) following the MD simulations and subsequent analyses with GROMACS (Figure 1).

3.2.TheResults of MD Simulation Analysis

MD simulation study was performed for each of the wild and mutant variants to identify the structural modification of F312Y mutation on the Cyc2 protein in a dynamic system. To perform a search for structural modifications due to mutation, RMSD, RMSF, Rg, SASA, H-bond, DSSP, Mean smallest distance, APL-thickness, PCA, ED, DCCM, FEL and EM were used. The results of RMSD, RMSF, Rg, SASA and H-bond show the stability of the protein structure after mutation (Figure S1, Table S1). The following images depict the modification of the Cyc2 protein secondary structure of both wild-type and F312Y mutant variants during the simulation (Figure 2).

Alterations in the protein's secondary structure during the simulations are illustrated in Figures 2A-C. The DSSP method was utilized to determine the content of secondary structural elements of proteins. Analysis of Cyc2 secondary structure at the outer membrane shows that each of β-sheets, bends, and 3_{10}-helices presented increases of +0.01. This was compensated by reduction of -0.02 and -0.01 in the contents of coils and β-bridges, respectively. According to the results, β-sheets, 3_{10}-helices, and bends were the dominant secondary structure elements in both systems (Table 2 and 3).

3.3. Principle Component Analysis (PCA)

The scatter graph constructed for the wild-type and F312Y mutant, as displayed in Figure 3, indicates a slight variation between the two systems. The overall movement of the two systems, as displayed in the graph, is similar. The molecular alterations are represented in the atomic density plot (Figure 3A).

Table 1. Prediction of protein stability changes upon point mutations at 30 ^{o}C and pH 2

Parameters / Predictor			
ΔΔG		Confidence Score	
DUET	I-Mutant2	MUpro	I-stable
0.062	-0.42	1	0.825

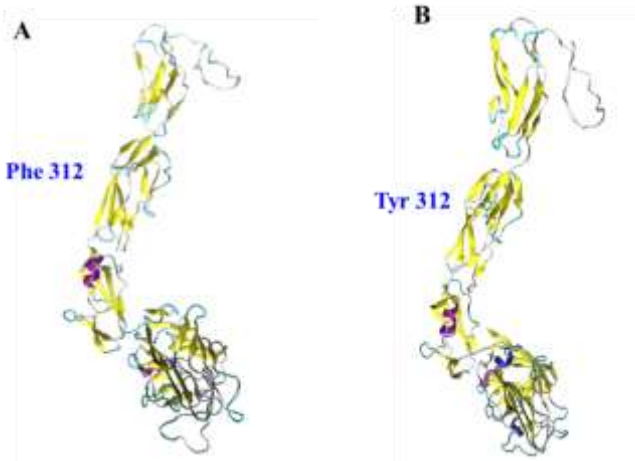

Figure 1. Structural model of Cyc2 (A) Structure of wild-type Cyc2 (cartoon model) and Phenylalanine (CPK model). (B) Structure of F312Y-mutant Cyc2 (cartoon model) and Tyrosine (CPK model).

Table 2. Percentage of secondary structure of wild and mutant protein (F312Y) during 100 ns of MD simulation

Secondary Structure (%) / Strain	Structure	Coil	β-sheet	β-Bridge	Bend	Turn	α-Helix	3_{10}-Helix
Wild-type	100	42	29	3	12	11	2	1
F312Y Mutant	100	40	30	2	13	11	2	2

Table 3. The average for the secondary structure of wild and F312Y mutant during 70 ns of MD simulation. The values of DSSP have been given in numbers

Secondary Structure	Structure	Coil	β-sheet	β-Bridge	Bend	Turn	A-Helix	3-Helix
Wild-type	100	93.33	62.22	6.66	26.66	24.44	4.44	2.22
F312Y Mutant	100	88.88	66.66	4.44	28.88	24.44	4.44	4.44

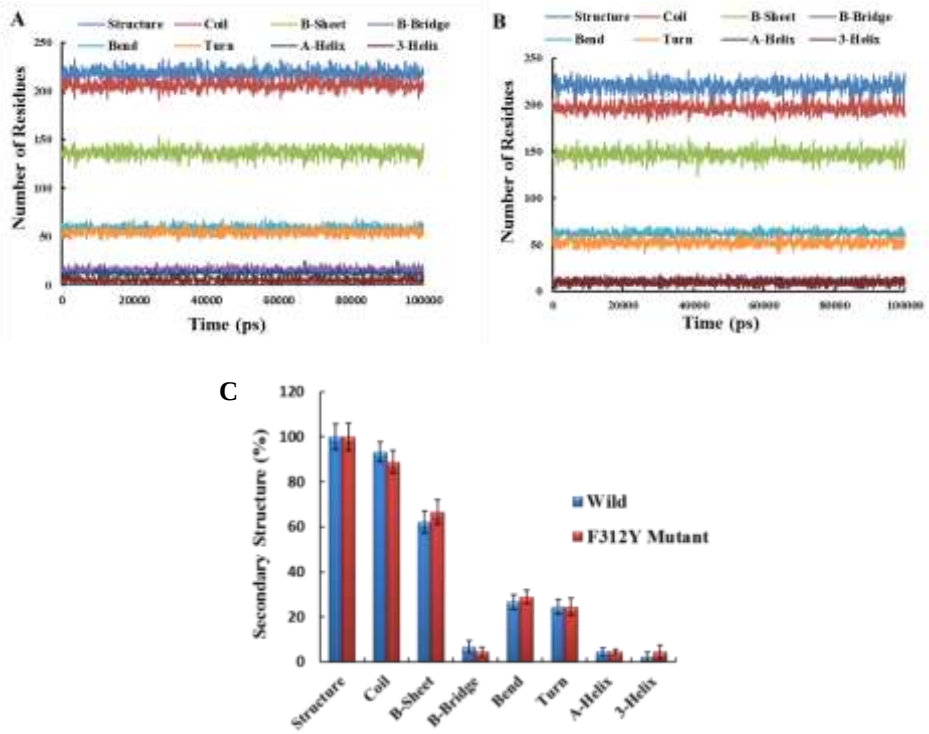

Figure 2. The wild-type secondary structure compared to the hot spot mutant form (F312Y). (A, B, and C) The DSSP timeline plots (70 ns) of wild-type and F312Y mutant systems at 300 K.

A slight variation in the density dispersal of the wild compared to the F312Y variant was observed. Besides, the mutant structure shows higher atomic density dispersal compared to the wild-type. Furthermore, the F312Y mutant complex populates an identical phase space and demonstrates a higher fluctuation compared to the wild-type. The Cross-correlation matrix and a plot of the correlated and anti-correlated movements in the wild- type and mutant systems are shown in Figure 3A. Particularly, F312Y single mutation produced an alteration in the profile of the cumulative correlation movements. This impact shows that a partial folding of the mutant protein area has primarily anti-correlated movement that is largely taking part in contact with other spheres.

3. 4. Essential Dynamics (ED)

Essential dynamics analysis of MD trajectories of the wild-type and F312Y mutant variant structures revealed that just a small number of eigenvectors have important eigenvalues (Figure 3B). Diagonalization of the covariance matrix indicated that the mutant system encountered a greater magnitude of fluctuation in the course of simulation. Specifically, every one of the first 3 eigenvectors has a greater eigenvalue during F312Y variant simulation relative to the wild-type simulation (Figure 3B). The upper triangle of the correlation map observes only cross-correlations larger than 0.5 (absolute values). Therefore, the upper triangle shows merely the most correlated motions.

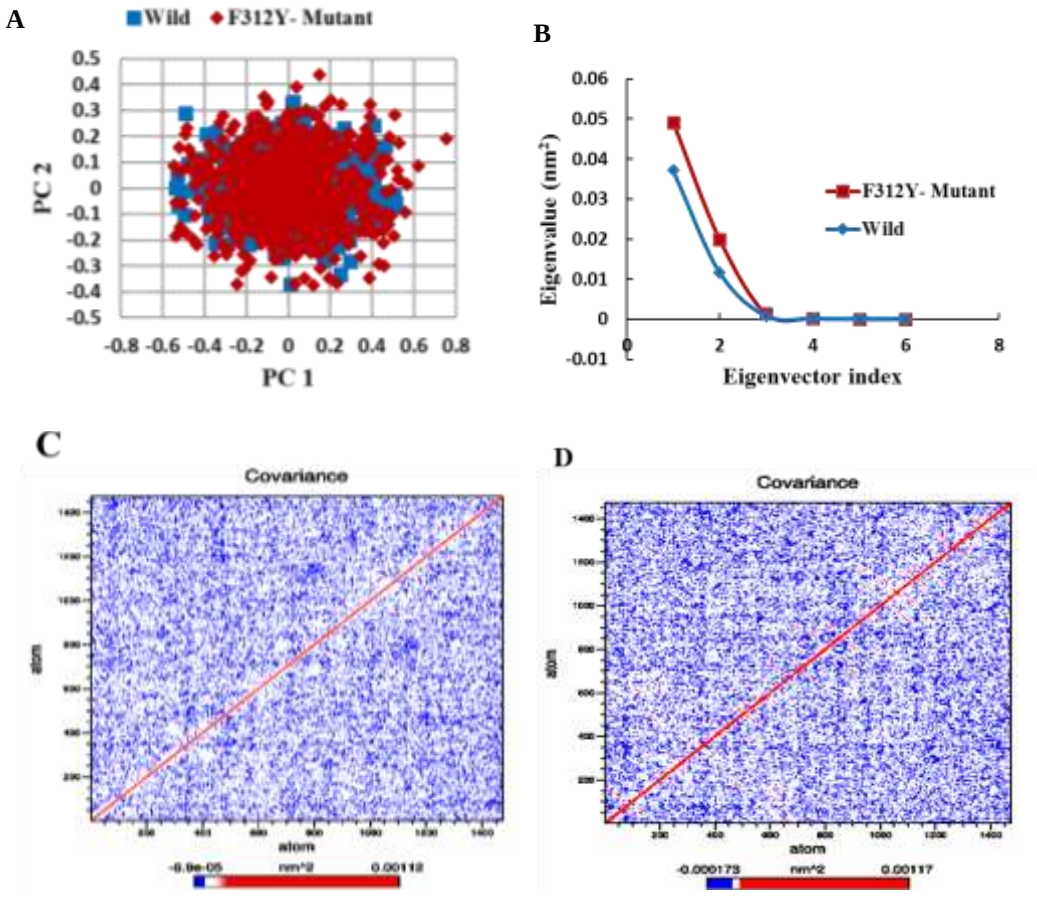

Figure 3. Dynamic consequences of the F312Y mutation on Cyc2. (A) PCA scatter plot of the first two principal components, PC1 and PC2. (B) Essential dynamics analysis. (C and D) Comparison of cross correlation matrices of wild-type (C) and mutant variant (D).

3. 5. Mutation Induced Changes in Hydrogen Bond Formation and Their Function in Dynamic Cross Correlation

In this study, the dynamic cross-correlation map (DCCM) was obtained for all the systems (Figure 3C and D) at 300 K.

The authors related their findings with the impact of mutation-induced stabilization (or destabilization) of hydrogen bonds on the protein. The color sequence goes from blue (-1) via white (0) to red (+1). The negative values are representative of anticorrelated displacements (in the opposite direction), while positive values represent correlated displacements (in the same direction). The overall reduction in the positive correlation, seen in the wild-type system, could be mainly due to the destabilization of several hydrogen bonds. The above-mentioned findings indicate that both F312Y and wild variants presented a reduction in the positive correlation. They also demonstrated that the higher positive correlation in different areas of the mutant can be ascribed to local (in F312Y) impacts of combined mutations developed from the stabilization of various sets of hydrogen bonds.

3. 6. Free Energy Landscape (FEL)

As shown in Figure 4, FEL was generated for all Cα of both systems. The study of FEL using the first and second principal components (PC1 and PC2) revealed ΔG values of 0 to 6.71 kJ/mol for the wild-type and 0 to 6.15 kJ/mol for F312Y mutant variant. The size and shape of the minimal energy surface (blue area) exhibit the stability of a system. Smaller and more condensed blue zones indicate a greater stability of the corresponding complex. The lowest energy for wild-type system was 0.28 kcal/mol and 0.256 kcal/mol for the mutant variant, revealing that F312Y mutation influences the overall conformational stability of the system (Figure 4A and B).

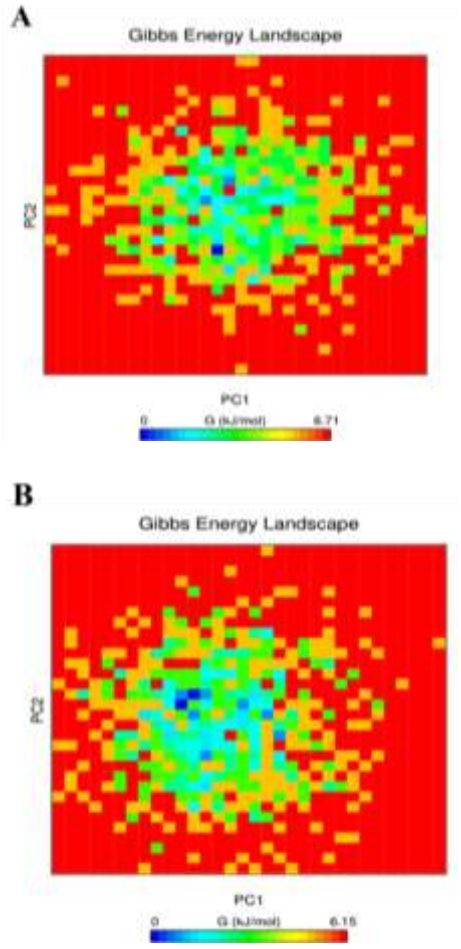

Figure 4. Free energy landscape of wild and F312Y mutant variant conformational space onto PC1 and PC2 obtained from PCA. Free energy landscape of the first two principal components (PC1, PC2) for wild (A) and mutant (B). Dark blue and red display the lowest and the highest energy configurations, respectively.

4. Discussion

Cyc2 is the first enzyme of the respiratory chain which transfers electrons across the external membrane to proteins like rusticyanin in the periplasmic space. Cytochrome c gains the electrons through the oxidation of Fe^{2+}. Molecular dynamics simulation of the wild-type and F312Y mutant variants revealed the effect of mutations at the atomic level. An analysis plan was used to calculate protein changes during the simulation. The trajectory analysis indicated minor changes in the protein's conformational stability.

Molecular dynamics simulation provided a chance to also assess the role of this mutation in the intermolecular interactions that enhance electron transfer efficiency.

Shojapour *et al*. indicated that Cyc and Cox are linked via water molecule No. 76, via two amino acids of His53 in Cyc, and Glu126 in Cox through hydrogen bonding. H53I mutation reduces the distance between isoleucine and water numbers 2030 and 2033 (which is below the protein toward CoxB). Therefore, reduces the distance between isoleucine and the water molecule 76 compared to histidine, resulting in a stronger hydrogen bond between the two proteins Cyc1 and CoxB (Shojapour *et al*., 2021). As a result, the electron transfer rate increased between Cyc2 and Rus (Gooley *et al*., 1992).

Increasing the H-band and decreasing the amount of both Rg and SASA indicates protein more compactness and greater structural stability. The changes in RMSD and RMSF are very small and did not affect protein instability (Er *et al*., 2011; Imani *et al*., 2018).

In the mean smallest distance analysis we have characterized the mean inter-chain contacts of both wild Cyc2 and F312Y mutant obtained from MD simulation. Only slight variations are observed in the interdomain contacts of α3 and α3 chains. Therefore the residue-residue contacts between wild Cyc2 and mutated F312Y do not show significant variations. From contact map analysis, it is obvious that contacts between residues are not disturbed in mutated F312Y indicates stabilization of Cyc2 structure after mutation (Imani *et al*., 2018). Our results were similar to Pahari and his *et al* research (Pahari *et al*., 2013).

The distribution of protein, protein-POPC and POPC atoms before and after mutation, indicated that the F312Y mutated protein structure occupied less space than the wild-type. This was a very small decrease. This was in parallel with the results of the alteration in the second structure of the protein after the mutation. By conversion of phenylalanine 312 into tyrosine, an α-amino acid with hydrophobic and nonpolar side chain is converted to an amino acid with a polar side group with an extra -OH group that ultimately increases intramolecular hydrogen bonds. Consequently, the structure of mutated proteins was more stable than the wild-type. Therefore, the protein structure can be relatively compact and occupy less space. In Rayapadi *et al*. study, it was observed that the mutated protein structure took up a slightly larger region than the wild-type after the D835N mutation in fetal liver tyrosine kinase 3 (FLT3). The results from the mentioned study indicated that after converting an acidic amino acid to a hydrophilic one, the density increased and the protein structure became slightly more open and therefore occupied more space (Swetha *et al*., 2016).

According to the secondary structure prediction studies, Cyc2 does not have any α-helices long enough to cross the internal membrane (IM) (Quatrini *et al*., 2006). It contains a known outer membrane beta-barrel domain, with an N-terminal expansion that probably has a small cytochrome-like domain containing a haem group. Phe312 receives an electron from haem C and gives it to Asp73 of rusticyanin. Therefore, based on the results from molecular dynamics simulations like Rg, SASA, Hbond, *etc.*, we can conclude that the protein is more compact and stable after the mutation. Moreover, the electron transfer rate between phenylalanine 312 of Cyc2 and Asp 73 of rusticyanin may increase. As a result, the bioleaching rate will probably increase. Furthermore, based on MD results, it can be predicted that the stability of the Cyc2 upon F231Y substitution will increase. Therefore, the affinity of the Cyc2- rusticyanin

interaction could be modified and biological function of Cyc2 as the main protein in the electron transfer further activated.

The stability and function of proteins are two important interdependent properties to consider in protein structure. Mutations that negatively affect either the stability or function of a protein directly affect the other. Hence, the stability of a protein plays a key role in maintaining its function (Sudhakar *et al*., 2016).

Essential dynamics analysis was performed on the wild-type and F312Y mutant variant. This analysis is applied to control the overall strenuous motions of the complex. Our results show that the overall motion between the two systems was similar. It meant that anti-correlated motions were observed in both systems. There is a significant difference between our results and the data from previous studies. Imani *et al*. demonstrated that leucine-to-proline substitution showed higher fluctuation compared to the wild-type (Imani *et al*., 2018). This was associated with two different types of amino acids in contrast to the present study, which addressed the substitution of similar amino acids (phenylalanine to tyrosine). Therefore, it can be deduced that attaining consistent distribution patterns between the wild-type and mutant variants is crucial. In order to compare the fluctuations of eigenvectors with eigenvalues in the wild and mutant systems, we used ED analyses of MD trajectories.

Since Cyc2 interacts with Asp73 of rusticyanin to transfer the electron in the respiratory system, we can suggest that the increase of the first 3 eigenvectors leads to improved flexibility and the potential binding affinity between Cyc2 and rusticyanin.

It is commonly acknowledged that the computational and theoretical methodologies, such as molecular dynamics simulation, PCA, and FEL, serve as valuable tools for assessing the effects of point mutations on protein function and structure (Martin *et al*., 2011).

To explore the local and universal physicochemical effects of the mutations on the conformational diversity and protein stability, we constructed the FELs of the wild and mutant systems in the course of simulation. Mutation of residues decreased the overall binding energy by ~0.6 kcal/mol in addition to modifying the landscape of the protein. Our results showed that mutation of the key residue near the binding site of rusticyanin influenced the overall conformational landscape of the system. Our results were not consistent with the Imlimaong Aier *et al*. study, because they assessed the impact of the mutation on the enhancer of zeste homolog 2 (EZH2). Mutation of residues improved the overall binding energy by ~ −0.6 kcal/mol. In addition, the mutation modified the landscape of the protein and the atomic interaction among the ligand-protein and the involved residues. Imlimaong Aier *et al*. (2016), maintained that the mutation of two key residues near the active site impacts the general conformational landscape of the system and consequently alters the interaction network. However, F312Y caused a decrease in free energy landscape or Gibbs energy during the simulation time. Therefore, the conformational structure of the protein can be more stable compared to the wild-type.

Also, the energy minimization (EM) value at position 312 in wild and mutant bacteria was 30.018 and -36.112, respectively. This decrease in EM after the mutation indicates greater stability of structure and the accuracy of other analyses (Xu and Zhang 2011).

Differences in redox oxidation potential in chain components lead to

electron transfer in the chain. There is a direct relationship between electron reception and the amount of oxidation potential (E_o). The amount of E_o is managed by axial ligand mutation (Thomann *et al*., 1991). Due to the change in the dielectric constant around the axial location, the E_o value changes. The increase of the E_o value is directly related to the attenuation of axial ligand interaction (Tyr312). Therefore, it can be said, a weak axial ligand (Tyr) enhancement the redox potential (Kanbi *et al*., 2002). In addition, the results of the RMSF analysis show an increase in the flexibility of the ligands after mutation, where Tyr312 had an increase in the RMSF value than the wild-type (F312= 0.01948, Y312= 0.01955). According to these results, the F312Y mutation reduces stability at the active site. Therefore, active site flexibility causes an increase in the value of E_o.

The increase in the flexibility of the ligands in the active site as well as the increase in the hydrophobicity parameter in this region indicates significant instability at the active site of the mutant protein (Jafarpour *et al*., 2020). Δs E_o increases at the point of mutation, the tendency to receive electrons from previous parts of the electron transfer chain, followed by the bioleaching efficiency of the bacterium, increases. According to the ΔG equation, the value of ΔG is inversely related to the value of ΔS (1).

$$\Delta G = \Delta H - T\Delta S \quad (1)$$

ΔG is the change in Gibbs free energy, ΔH is the change in internal energies, T is the temperature in Kelvin and ΔS is the change in ligand flexibility and increasing with ΔG decreases. Also, according to the Nernst equation, the redox potential (E_o) is related to the change in free energy (ΔG) between the reactant and the product state in the redox reaction (Li *et al*., 2015).

$$Eg = -\Delta G/nF \quad (2)$$

Where n is the number of electrons transferred and F is the Faraday constant (2). Thus, the calculation of the redox potential is correlated to the calculation of the free energy change. By decreasing ΔG, the amount of redox potential increases, and electron transfer and bioleaching are improved.

5. Conclusions

In general, the analysis results (hydrogen bonds, DSSP, mean smallest distance, density, RMSD, RMSF, Rg, SASA, H-bond, PCA, ED, DCCM, FEL, and EM) show that the protein structure has become more compact after the mutation (F312Y). The folding of the protein indicates its stability after mutation. Also, the stability of a protein plays a key role in maintaining its function. Comparison between previous studies and our research revealed the importance of tryptophan, tyrosine, and phenylalanine in electron transmission.

The results of RMSF analysis were followed by increased E_o, and a more tendency to receive electrons. For future studies on mutation, we propose a careful investigation of electron transfer improvement through QM/MM calculations, as well as determine the E_o changes of mutant protein using MD and QM computational methods. Moreover, selecting the optimal mutant identified via bioinformatics methods could facilitate the cloning of bacteria with mutations, thereby enhancing the bioleaching process.

Author Contributions

Conceptualization, S.S., M.D., M.SH., and F.F.; methodology, S.S., M.D., and M.SH.; software, S.S., and M.SH.; validation, M.D., and F.F.; formal analysis, S.S., M.D., and M.SH.; investigation, M.SH., and S.F.; resources, S.F.; data curation, S.S., and M.D., writing—original draft preparation, S.S.,

M.D., and M.SH.; writing-review and editing, S.S., and M.D., visualization, S.S., and M.D., supervision, S.S., and M.D., project administration, M.D.; funding acquisition, S.S., and M.SH., All authors have read and agreed to the published version of the manuscript.

Acknowledgements
The authors thank Ms. Saba Miri for her valuable technical advice.

Abbreviations
F312Y	Phenylalanine 312 Tyrosine
OM	Outer Membrane
Af	*Acidithiobacillus ferrooxidans*
cytC	Cytochrome c
MD	Molecular Dynamic Simulations
RMSD	Root-mean-square deviation
RMSF	Root-mean-square fluctuation
SASA	Solvent-accessible surface area
Rg	Radius of gyration
H Bond	Hydrogen Bonds
DSSP	Define Secondary Structure of Proteins
PCA	Principal Component Analysis
ED	Essential Dynamics
DCCM	Dynamic Cross Correlation Map
FEL	Free Energy Landscape
EM	Energy Minimization
SEM	Standard Error of the Mean
QM/MM	Quantum Mechanics/Molecular Mechanics
E_o	Oxidation Potential
ΔG	Free Energy
IMP	Integral Membrane protein
PC	Principal Components

Declaration of competing interest
No potential conflict of interest was reported by the authors.

Data Availability
Data will be made available on request.

References
Abriata, L. A. (2018). Structural model of Cyc2, the primary electron acceptor of Acidithiobacillus ferrooxidans' respiratory chain, as a modular cytochrome-β-barrel fusion protein, and mechanistic proposals based on this model. bioRxiv, 262287. https://doi.org/10.1101/262287.

Aier, I., Varadwaj, P. K., & Raj, U. (2016). Structural insights into conformational stability of both wild-type and mutant EZH2 receptor. Scientific reports, 6(1), 1-10. https://doi.org/10.1038/srep34984.

Amadei, A., Linssen, A. B., & Berendsen, H. J. (1993). Essential dynamics of proteins. Proteins: Structure, Function, and Bioinformatics, 17(4), 412-425. https://doi.org/10.1002/prot.340170408

Balsera, M. A., Wriggers, W., Oono, Y., & Schulten, K. (1996). Principal component analysis and long time protein dynamics. The Journal of Physical Chemistry, 100(7), 2567-2572. https://doi.org/10.1021/jp9536920

Bekker, H., Berendsen, H. J. C., Dijkstra, E. J., Achterop, S., Vondrumen, R., Vanderspoel, D., ... & Renardus, M. K. R. (1993). Gromacs-a parallel computer for molecular-dynamics simulations. In 4th international conference on computational physics (PC 92) (pp. 252-256). World Scientific Publishing. https://research.rug.nl/en/publications/gromacs-a-parallel-computer-for-molecular-dynamics-simulations

Berendsen, H. J., Postma, J. P., van Gunsteren, W. F., & Hermans, J. (1981). Interaction models for water in relation to protein hydration. In Intermolecular forces: proceedings of the fourteenth Jerusalem symposium on quantum chemistry and biochemistry held in jerusalem, israel, 11(1), 331-342. Springer Netherlands. https://doi.org/10.1007/978-94-015-7658-1_21

Berendsen, H. J., Postma, J. V., Van Gunsteren, W. F., DiNola, A. R. H. J., & Haak, J. R. (1984). Molecular dynamics with coupling to an external bath. The Journal of chemical physics, 81(8), 3684-3690. https://doi.org/10.1063/1.448118.

Berendsen, H. J., van der Spoel, D., & van Drunen, R. (1995). GROMACS: A message-passing parallel molecular dynamics implementation. Computer physics communications, 91(1-3), 43-56. https://doi.org/10.1016/0010-4655(95)00042-E.

Capriotti, E., Fariselli, P., & Casadio, R. (2005). I-Mutant2. 0: predicting stability changes upon mutation from the protein sequence or structure. Nucleic acids research, 33(2), 306-310. https://doi.org/10.1093/nar/gki375.

Chen, C. W., Lin, J., & Chu, Y. W. (2013). iStable: off-the-shelf predictor integration for predicting protein stability changes. In BMC bioinformatics, 14(2) 1-14. BioMed Central. https://doi.org/10.1186/1471-2105-14-S2-S5.

Cheng, J., Randall, A., & Baldi, P. (2006). Prediction of protein stability changes for single-site mutations using support vector machines. Proteins: Structure, Function, and Bioinformatics, 62(4), 1125-1132. https://doi.org/10.1002/prot.20810.

De Groot, B. L., Amadei, A., Scheek, R. M., Van Nuland, N. A. J., & Berendsen, H. J. C. (1996). An extended sampling of the configurational space of HPr from E. coli. Proteins: Structure, Function, and Bioinformatics, 26(3), 314-322. https://doi.org/10.1002/(SICI)1097-0134(199611) 26:3<314::AID-PROT7>3.0.CO;2-D

Er, T. K., Chen, C. C., Liu, Y. Y., Chang, H. C., Chien, Y. H., Chang, J. G., ... & Jong, Y. J. (2011). Computational analysis of a novel mutation in ETFDH gene highlights its long-range effects on the FAD-binding motif. BMC structural biology, 11(1), 1-11. https://doi.org/10.1186/1472-6807-11-43.

Faraldo-Gómez, J. D., Smith, G. R., & Sansom, M. S. (2002). Setting up and optimization of membrane protein simulations. European Biophysics Journal, 31, 217-227. https://doi.org/10.1007/s00249-002-0207-5.

Ghasemi, F., Zomorodipour, A., Karkhane, A. A., & Khorramizadeh, M. R. (2016). In silico designing of hyper-glycosylated analogs for the human coagulation factor IX. Journal of Molecular Graphics and Modelling, 68(1), 39-47. https://doi.org/10.1016/j.jmgm.2016.05.011

Gooley, P. R., Caffrey, M. S., Cusanovich, M. A., & MacKenzie, N. E. (1992). Mutations Pro. fwdarw. Ala-35 and Tyr. fwdarw. Phe-75 of Rhodobacter capsulatus ferrocytochrome c2 affect protein backbone dynamics: measurement of individual amide proton exchange rate constants by proton-nitrogen-15 HMQC spectroscopy. Biochemistry, 31(2), 443-450. https://doi.org/10.1021/bi00117a020.

Hess, B., Bekker, H., Berendsen, H. J., & Fraaije, J. G. (1997). LINCS: A linear constraint solver for molecular simulations. Journal of computational chemistry, 18(12), 1463-1472. https://doi.org/10.1002/(SICI)1096-987X(199709)18:12<1463::AID-JCC4>3.0.CO;2-H

Ichiye, T., & Karplus, M. (1991). Collective motions in proteins: a covariance analysis of atomic fluctuations in molecular dynamics and normal mode simulations. Proteins: Structure, Function, and Bioinformatics, 11(3), 205-217. https://doi.org/10.1002/prot.340110305.

Imani, S., Cheng, J., Shasaltaneh, M. D., Wei, C., Yang, L., Fu, S., ... & Fu, J. (2018). Genetic identification and molecular modeling characterization reveal a novel PROM1 mutation in Stargardt4-like macular dystrophy. Oncotarget, 9(1), 122. doi: 10.18632/oncotarget.22343.

Imani, S., Ijaz, I., Shasaltaneh, M. D., Fu, S., Cheng, J., & Fu, J. (2018). In silico data analyses of the hotspot mutations of CHM gene in choroideremia disease. Data in brief, 18(1), 1217-1223. https://doi.org/10.1016/j.dib.2018.04.023.

Jafari, M., & Mehrnejad, F. (2016). Molecular insight into human lysozyme and its ability to form amyloid fibrils in high concentrations of sodium dodecyl sulfate: a view from molecular dynamics simulations. PLoS One, 11(10), e0165213. https://doi.org/10.1371/journal.pone.0165213

Jafarpour, R., Fatemi, F., Eidi, A., & Mehrnejad, F. (2021). Effect of the Met148Leu mutation on the structure and dynamics of the rusticyanin protein from Acidithiobacillus sp. FJ2. Journal of Biomolecular Structure and Dynamics, 39(11), 4122-4132. https://doi.org/10.1080/07391102.2020.1775119.

Kanbi, L. D., Antonyuk, S., Hough, M. A., Hall, J. F., Dodd, F. E., & Hasnain, S. S. (2002). Crystal structures of the Met148Leu and Ser86Asp mutants of rusticyanin from Thiobacillus ferrooxidans: insights into the structural relationship with the cupredoxins and the multi copper proteins. Journal of molecular biology, 320(2), 263-275. https://doi.org/10.1016/S0022-2836(02)00443-6.

Kolling, D. J., Brunzelle, J. S., Lhee, S., Crofts, A. R., & Nair, S. K. (2007). Atomic resolution structures of rieske iron-sulfur protein: role of hydrogen bonds in tuning the redox potential of iron-sulfur clusters. Structure, 15(1), 29-38. https://doi.org/10.1016/j.str.2006.11.012.

Li, W., Baldus, I. B., & Gräter, F. (2015). Redox potentials of protein disulfide bonds from free-energy calculations. The Journal of Physical Chemistry B, 119(17), 5386-5391. https://doi.org/10.1021/acs.jpcb.5b01051.

Lindahl, E., Hess, B., & Van Der Spoel, D. (2001). GROMACS 3.0: a package for molecular simulation and trajectory analysis. Molecular modeling annual, 7(1), 306-317. https://doi.org/10.1007/s008940100045.

Lyons, J. A., Aragão, D., Slattery, O., Pisliakov, A. V., Soulimane, T., & Caffrey, M. (2012). Structural insights into electron transfer in caa 3-type cytochrome oxidase. Nature, 487(7408), 514-518. https://doi.org/10.1038/nature11182.

Martin, A. J., Vidotto, M., Boscariol, F., Di Domenico, T., Walsh, I., & Tosatto, S. C. (2011). RING: networking interacting residues, evolutionary information and energetics in protein structures. Bioinformatics, 27(14), 2003-2005. https://doi.org/10.1093/bioinformatics/btr191

Pahari, B., Chakraborty, S., Sengupta, B., Chaudhuri, S., Martin, W., Taylor, J., ... & Sengupta, P. K. (2013). Biophysical characterization of genistein in its natural carrier human hemoglobin using spectroscopic and computational approaches, 4(8A), 35277-35287. doi:10.4236/fns.2013.48A011.

Patra, M. C., Pradhan, S. K., Rath, S. N., & Maharana, J. (2013). Structural analysis of respirasomes in electron transfer pathway of Acidithiobacillus ferrooxidans: a computer-aided molecular designing study. International Scholarly Research Notices, 95718-95732 http://dx.doi.org/10.1155/2013/295718.

Pearlman, D. A., Case, D. A., Caldwell, J. W., Seibel, G. L., Singh, U. C., Weiner, P., & Kollman, P. A. (1991). AMBER, a package of computer programs for applying molecular mechanics, normal mode analysis, molecular dynamics and free energy calculations to simulate the structural and energetic properties of molecules. 91(1-3), 1-41. https://doi.org/10.1016/0010-4655(95)00041-D.

Pires, D. E., Ascher, D. B., & Blundell, T. L. (2014). mCSM: predicting the effects of mutations in proteins using graph-based signatures. Bioinformatics, 30(3), 335-342. https://doi.org/10.1093/bioinformatics/btt691

Quatrini, R., Appia-Ayme, C., Denis, Y., Ratouchniak, J., Veloso, F., Valdes, J., ... & Bonnefoy, V. (2006). Insights into the iron and sulfur energetic metabolism of Acidithiobacillus ferrooxidans by microarray transcriptome profiling. Hydrometallurgy, 83(1-4), 263-272. https://doi.org/10.1016/j.hydromet.2006.03.030

Shojapour, M., Fatemi, F., Farahmand, S., & Shasaltaneh, M. D. (2021). Investigation of Cyc1 protein structure stability after H53I mutation using computational approaches to improve redox potential. Journal of Molecular Graphics and Modelling, 105(1), 107864. https://doi.org/10.1016/j.jmgm.2021.107864

Sudhakar, N., George Priya Doss, C., Thirumal Kumar, D., Chakraborty, C., Anand, K., & Suresh, M. (2016). Deciphering the impact of somatic mutations in exon 20 and exon 9 of PIK3CA gene in breast tumors among Indian women through molecular dynamics approach. Journal of Biomolecular Structure and Dynamics, 34(1), 29-41. https://doi.org/10.1080/07391102.2015.1007483.

Swetha, R. G., Ramaiah, S., & Anbarasu, A. (2016). Molecular dynamics studies on D835N mutation in FLT3—its impact on FLT3 protein structure. Journal of Cellular Biochemistry, 117(6), 1439-1445. https://doi.org/10.1002/jcb.25434.

Thomann, H., Bernardo, M., Baldwin, M. J., Lowery, M. D., & Solomon, E. I. (1991). Pulsed ENDOR study of the native and high pH perturbed forms of the blue copper site in stellacyanin. Journal of the American Chemical Society, 113(15), 5911-5913. https://doi.org/10.1021/ja00015a083.

Valdés, J., Pedroso, I., Quatrini, R., Dodson, R. J., Tettelin, H., Blake, R., ... & Holmes, D. S. (2008). Acidithiobacillus ferrooxidans metabolism: from genome sequence to industrial applications. BMC genomics, 9(1), 1-24. https://doi.org/10.1186/1471-2164-9-597.

Van Der Spoel, D., Lindahl, E., Hess, B., Groenhof, G., Mark, A. E., & Berendsen, H.J. (2005). GROMACS: fast, flexible, and free. Journal of computational chemistry, 26(16), 1701-1718. https://doi.org/10.1002/jcc.20291.

Xu, D., & Zhang, Y. (2011). Improving the physical realism and structural accuracy of protein models by a two-step atomic-level energy minimization. Biophysical journal, 101(10), 2525-2534. https://doi.org/10.1016/j.bpj.2011.10.024

Yarzábal, A., Brasseur, G., Ratouchniak, J., Lund, K., Lemesle-Meunier, D., DeMoss, J. A., & Bonnefoy, V. (2002). The high-molecular-weight cytochrome c Cyc2 of Acidithiobacillus ferrooxidans is an outer membrane protein. Journal of Bacteriology, 184(1), 313-317. https://doi.org/10.1128/JB.184.1.313-317.2002.